Int J Adv Manuf Technol (2015) 76:691–703
DOI 10.1007/s00170-014-6291-8

ORIGINAL ARTICLE

Empirical models for cutting forces in finish dry hard turning of hardened tool steel at different hardness levels

Linhu Tang · Zhongwen Cheng · Jianlong Huang · Chengxiu Gao · Wenchun Chang

Received: 17 January 2013 / Accepted: 19 August 2014 / Published online: 5 September 2014

Abstract In this research, the exponential and quadratic polynomial empirical models for three-component cutting forces by employing five factors, such as the cutting speed, depth of cut, feed, workpiece hardness, and nose radius, were developed by utilizing the orthogonal regression methodology (ORM) and response surface methodology (RSM). On the other hand, an attempt has been made to experimentally investigate the effects of those factors on three-component cutting forces in finish dry hard turning (FDHT) of tool steel AISI D2 with the PCBN tool. In this investigation, based on five-factor three-level orthogonal experiments, three-component cutting forces were measured, and then, analysis of variance (ANOVA) was performed to estimate the significance of developed models and analyze the main and interaction effects of the factors. The experimental results indicated that the RSM quadratic polynomial empirical model (RSMQPEM) is much more accurate and credible than the ORM exponential empirical model (ORMEM) in predicting the three-component cutting forces. It was also found that the cutting speed and feed are the two dominant factors affecting the main cutting forces F_Z; the feed is the one dominant factor affecting radial cutting force F_Y and the feed cutting force F_X. Additionally, the optimum cutting parameters for the hardened materials with 51, 55, 60, and 64 HRC was found.

L. Tang (✉) · Z. Cheng · C. Gao · W. Chang
Provincial Key Laboratory for Green Cutting Technology and Application of Gansu Province (University), Lanzhou Institute of Technology, Gongjiaping East Road, 730050 Lanzhou, Gansu Province, People's Republic of China
e-mail: tanglinhu@126.com

J. Huang
College of Mechano-Electronic, Lanzhou University of Technology, 287 Langongping Road, 730050 Lanzhou, Gansu Province, People's Republic of China

Keywords Hardened tool steel · FDHT · Three-component cutting forces · ORM · RSM · ANOVA · RSMQPEM · ORME · M

Nomenclature

v	Cutting speed (m/min)
a_p	Depth of cut (mm)
f	Feed (mm/rev)
H	Workpiece hardness (HRC)
r_ε	Nose radius (mm)
b	Chamfer width
β	Chamfer angle (°)
F_X	Feed cutting force (N)
F_Y	Radial cutting force (N)
F_Z	Main cutting force (N)
κ_r	Major cutting-edge angle (°)
κ_r'	End-cutting edge angle (°)
a	Rake angle (°)
γ_0	Clearance angle (°)
γ_0'	Side clearance angle (°)
λ_s	Inclination angle (°)

1 Introduction

The hard turning is defined as the single-point turning process of materials with hardness greater than 45 Rockwell Hardness measured on the C scale (HRC) under appropriate cutting tools [1]. It has gained more attention owing to its substantial advantages, such as reducing time of finish machining, declining cost of manufacturing, and offsetting the environment concerns compared to grinding [2–4].

Therefore, numerous investigations have been carried out to study the tool life, surface integrity, and the cutting forces in turning operations. One of those studies is to focus on the empirical models about the cutting forces. Tang et al. [5] have investigated the effect of the effects of cutting speed, depth of cut, feed, workpiece hardness (51, 55, 58, 62, and 65±1 HRC), tool flank wear, and nose radius on cutting forces and not established the empirical models for cutting forces. More et al. [6] have analyzed the effect of cutting speed and feed on cutting forces using an analysis of variance (ANOVA) technique. Sharma et al. [7] utilized a neural network to construct a model in finish hard turning. Then, the model obtained was tested with the experimental data. Gaitonde et al. [1] analyze the effects of depth of cut and machining time on machining force using second-order mathematical models in turning of AISI D2 tool steel. Sieben [8] have established the empirical model for cutting forces based on such parameters as cutting speed, feed, and depth of cut. Based on Taguchi's method, the empirical model for cutting forces in the hard milling of AISI H13 steel has been developed by Ding et al. [9]. Gopalsamy [10] have studied the performance characteristics of machining process parameters, such as cutting speed, feed, depth of cut, and width of cut by utilizing an orthogonal array and ANOVA and then obtained optimum process parameters by gray relational analysis. Fnides et al. [11] have established statistical models of the cutting forces in hard turning of AISI H11 hot work tool steel and analyzed the effect of the main cutting variables, such as cutting speed, feed, and depth of cut on cutting force components. Besides, Aouici et al. [12] have experimentally investigated the effects of cutting speed, feed rate, workpiece hardness, and depth of cut on cutting force in hard turning of AISI H11 steel (40, 45, and 50 HRC); then, mathematical model for cutting force components was developed by using the response surface methodology (RSM).

It is revealed from the literature reviewed above that the models proposed by scholars were mainly focused on the influence of cutting speed, depth of cut, and feed. In fact, there are a large number of parameters which affect the cutting forces. These include cutting tool variables, workpiece material variables, cutting conditions, etc. Therefore, the influence of these process parameters on the models and analyses of the effect are limited. Here, a study aims to develop models for cutting forces and investigate the effect of process parameters, such as cutting speed, depth of cut, feed, hardness of workpiece, and nose radius, using the orthogonal regression methodology (ORM) and RSM approach. Then, ANOVA is performed to estimate the significance of developed models and analyze the main and interaction effects of factors.

2 Experimental details

2.1 Workpiece

In this study, the bar of tool steel AISI D2 (Cr12MoV, China) was used. The chemical composition is presented in Table 1. The bars of 48-mm diameter and 300-mm length were used.

Table 1 Chemical composition of the tool steel AISI D2 (wt%)

C	Cr	Mo	Mn	Si	P	S	V
1.55	11.25	0.45	0. 35	0.35	0.025	0.025	0.20

2.2 Heat treatment

In order to effectively utilize the finish dry hard turning (FDHT) process in the manufacturing industries, the hardened tool steel at different hardness levels was considered for the study with a polycrystalline cubic boron nitride (PCBN) insert. The results showed that the tool steel AISI D2 could get fine-needle martensite and high-diffusion and uniform distribution fine-grain carbide if using the quenching temperatures of 1,000–1,040 °C[13]. According to the methods of heat treatment in the literature [14], the specimens were put into an electrical resistance furnace at 1,000–1,040 °C, then quenched in oil, and finally tempered at various low temperatures. The obtained hardened specimens were in different hardness levels of 51±1, 58±1, and 64±1 HRC.

2.3 PCBN cutting tool

2.3.1 Choice of the contents of CBN

At present, in the tool and die industries, the PCBN tool has been extensively utilized to dry hard machine-hardened steel, refractory steel, and high-temperature alloy steel, specially for difficult-cut materials with the hardness of 55–65 HRC [15, 16].

In this paper, according to this literature [17], the PCBN cutting tools (type: GE2100, America) which had an approximate chemical composition of 50% CBN by volume and a CBN grain size of 2 μm were selected to turn the hardened tool steels at different hardness levels (51–64 HRC). In hard cutting, the carbide provides shock resistance; the CBN provides very high wear resistance and cutting-edge strength. Therefore, the composite PCBN inserts (type: SCGN150404) made in Beijing World Company were utilized to finish dry hard turn, as shown in Fig. 1.

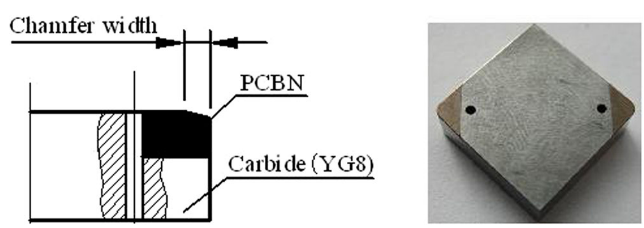

(a) Construction of a PCBN insert (b) PCBN insert

Fig. 1 Design schematic of a composite PCBN insert. **a** Construction of a PCBN insert. **b** PCBN insert

2.3.2 Geometry parameter of the PCBN tool

The inserts were clamped in a piezoelectric three-component turning dynamometer (type: YDC-III89A) tool holder. Except for the nose radius, all the composite PCBN inserts used for the experiments had the same tool geometry. The effective geometry parameters of PCBN cutting tool are presented in Table 2.

2.4 Experimental setups and procedures

2.4.1 Test system of cutting force

FDHT tests were conducted at room temperature of about 22 °C and relative humidity of about 40 %. A schematic of an FDHT setup and force measurement system is presented in Fig. 2. The piezoelectric three-component turning dynamometer was mounted on a CNC lathe in which speed can vary from 0 to 2,200 rpm and there is a maximum power of 9.5 kW, as shown in Fig. 3.

The test system of cutting forces was made up of a computer installed with Windows XP 2003 Professional and GDFMS dynamic measurement software for cutting forces, multifunctional data acquisition card (type: PCI-9118DG), multichannel charge amplifier (type: YE5850), and piezoelectric quartz crystal three-component force dynamometer (type: YDC-III89A).

2.4.2 Cutting force measurements

Three-component cutting force's signals obtained from the dynamometer were transferred to a computer by means of the multifunctional data acquisition card and then were evaluated by utilizing the GDFMS dynamic measurement software. In order to acquire exact cutting force, three-component forces were acquired during steady-state phase in FDHT. Each test was repeated for three times, and the mean cutting force was used for further analysis.

2.5 Experimental design

Turning is a complex process because many parameters, such as cutting speed, depth of cut, feed, tool geometry, workpiece material condition, turning environment, etc. are involved. In this study, five parameters, including cutting speed (v), depth of cut (a_p), feed (f), workpiece hardness (H), and nose radius (r_ε), were taken into consideration for conducting the experiments. Three levels were defined for each cutting variable as given in Table 3. Orthogonal design of experiments was utilized to design the experimentation. Therefore, the L27 $(3)^5$ (three levels-five factors) orthogonal array for this experimentation led to a total of 27 tests.

RSM is a type of modeling to develop the relationship between various factors with the response [18, 19]. It is an effective technique to design the experiments and analyze problems by applying ANOVA and regression analysis. The established empirical models for three-component cutting forces describe the interaction of various parameters with respect to response factors.

Table 2 The effective geometry parameters of the PCBN cutting tool

κ_r (°)	κ_r' (°)	α (°)	γ_0 (°)	$\gamma'0$ (°)	λ_s (°)	r_ε (mm)	β(°)	b (mm)
65	25	−5	5	5	−3	0.8, 1.2, 1.6	−15	0.1

3 Analysis and discussions

The experimental layout and experimental results of three-component cutting forces (F_X, F_Y, and F_Z) are presented in Table 4.

3.1 Modeling process

3.1.1 Method of the ORM exponential empirical model (ORMEM)

The functions of representing the three-component cutting forces can be expressed as [20]

$$F_X = C_X v^{l_X} a_p{}^{m_X} f^{n_X} H^{p_X} r_\varepsilon^{q_X} \tag{1}$$

$$F_Y = C_Y v^{l_Y} a_p{}^{m_Y} f^{n_Y} H^{p_Y} r_\varepsilon^{q_Y} \tag{2}$$

$$F_Z = C_Z v^{l_Z} a_p{}^{m_Z} f^{n_Z} H^{p_Z} r_\varepsilon^{q_Z} \tag{3}$$

where C_X, C_Y, and C_Z are respectively the correction coefficient of F_X, F_Y, and F_Z. l_X, m_X, n_X, p_X, and q_X; l_Y, m_Y, n_Y, p_Y, and q_Y; and l_Z, m_Z, n_Z, p_Z, and q_Z are exponents of corresponding parameters (v, ap, f, H, and $r\varepsilon$) in the ORMEM F_X, F_Y, and F_Z.

In order to make this paper concise, here, we only introduce the modeling process of the main cutting force F_Z.

Equation (3) may be transformed into the following linear model equation [21]:

$$\ln F_Z = \ln C_Z + l_Z \ln v + m_z \ln a_p + n_z \ln f + p_Z \ln H + q_Z \ln r_\varepsilon \tag{4}$$

Suppose

$$y = \ln F_z, b_0 = \ln C_z, x_1 = \ln v, x_2 = \ln a_p, x_3 = \ln f, x_4 = \ln H, x_5 = \ln r_\varepsilon; b_1 = l_Z, b_2 = m_Z, b_3 = n_Z, b_4 = p_Z, b_5 = q_Z$$

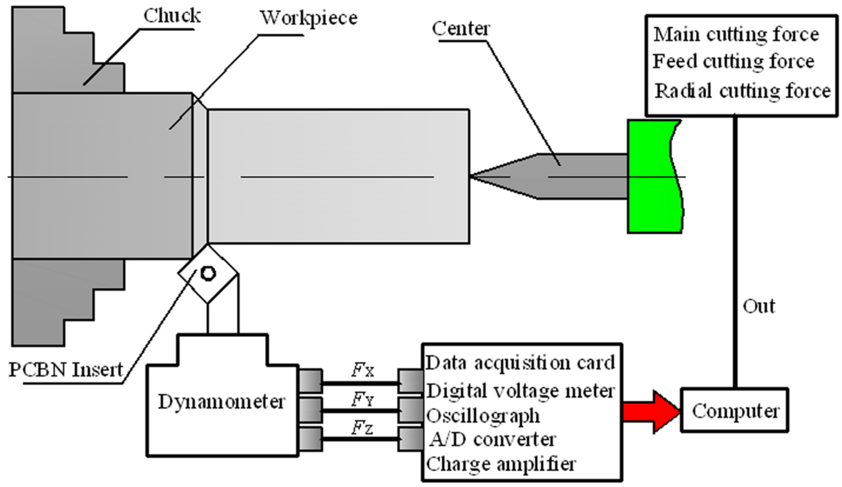

Fig. 2 Schematic of an FDHT setup and force measurement system

Thus, Eq. (4) becomes

$$y = b_0 + b_1x_1 + b_2x_2 + b_3x_3 + b_4x_4 + b_5x_5 \tag{5}$$

If there are m influential factors and n tests were conducted, then a multiple linear regression model can be generally described as [22, 23]

$$y = \beta_0 + \beta_1x_{i1} + \beta_2x_{i2} + \cdots + \beta_mx_{im} + \varepsilon_i, i \tag{6}$$

where β_0, β_1, and β_m are the predictable variables and x_1, x_2, and x_m are strictly controlled the natural elements. ε_1, ε_2, and ε_n are random variables which are independent mutually and obey the same normal distribution $N(0, \sigma^2)$.

If defined,

$$\mathbf{y} = \begin{pmatrix} y_1 \\ y_2 \\ \vdots \\ y_n \end{pmatrix}, \ \mathbf{x} = \begin{pmatrix} 1 & x_{11} & x_{12} & \cdots & x_{1m} \\ 1 & x_{21} & x_{22} & \cdots & x_{2m} \\ \vdots & \vdots & \vdots & & \vdots \\ 1 & x_{n1} & x_{n3} & \cdots & x_{nm} \end{pmatrix} \boldsymbol{\beta} = \begin{pmatrix} \beta_0 \\ \beta_1 \\ \vdots \\ \beta_m \end{pmatrix} \varepsilon = \begin{pmatrix} \varepsilon_1 \\ \varepsilon_2 \\ \vdots \\ \varepsilon_n \end{pmatrix}$$

A multiple linear regression model is represented in matrix form, which is generally described as

$$y = x\beta + \varepsilon \tag{7}$$

In linear regression analysis, Eq. (6) can be expressed as

$$\hat{y} = b_0 + \sum_{j=1}^{m} b_jx_j\hat{y}j \tag{8}$$

The least-squares estimate of regression coefficient β is generally described as [22]

$$b = \left(x^{\mathbf{T}}x\right)^{-1}\left(x^{\mathbf{T}}y\right) \tag{9}$$

3.1.2 Method of RSM quadratic polynomial empirical model (RSMQPEM)

In a general case, a second-order polynomial empirical model used to represent the response surface for k factors is given by [24]

$$y = \beta_0 + \sum_{i=1}^{k} \beta_ix_i + \sum_{i=1}^{k} \beta_{ii}x_i^2 + \sum_{i} \sum_{j\neq i}^{k} \beta_{ij}x_ix_j + \varepsilon \tag{10}$$

Fig. 3 FDHT

Table 3 Assignment of the levels to the variables

Level	v (m/min)	a_p (mm)	f (mm/rev)	H (HRC)	r_ε (mm)
1	75	0'.10	0.10	51±1	0.8
2	150	0.20	0.20	58±1	1.2
3	226	0.30	0.30	64±1	1.6

In the above equation, the β_0, β_i, β_{ii}, and β_{ij} are the regression coefficients and the residual; ε measures the experimental error of the nth observations.

In the case of engineering problems, higher order interactions, such as interactions of three or more factors, are not practically of significance. Thus, three and four factor interactions are ignored in the empirical model. The simplified model is a polynomial which is described as

$$y = \beta_0 + \beta_1(A) + \beta_2(B) + \beta_3(C) + \beta_4(D) + \beta_5(E) + \beta_6(AB) + \beta_7(AC)\beta_8(AD) + \beta_9(AE) + \beta_{10}(BC) + \beta_{11}(BD) + \beta_{12}(BE) + \beta_{13}(CD) + \beta_{14}(CE) + \beta_{15}(DE) \quad (11)$$

where β_0 is a constant; β_0, β_1, and β_{15} are coefficients based on the main as well as interaction effects.

3.1.3 Test of regression coefficient

The significance of the regression equation does not imply that each of the independent variables has a significant effect. Apparently, if the effect of a certain independent variable x_j on y is not significant, its coefficient β_j may equal to zero in this regression model. Therefore, whether a tested variable is significant or not is equivalent to hypothesis of testing shown in Eq. (12):

$$H_0 : \beta_j = 0 \quad (12)$$

Table 4 Experimental results for three-component cutting forces

Cr12MoV	Factors					Experimental results		
Tests	A v (m/min)	B a_p(mm)	C f (mm/rev)	D H (HRC)	E r_ε (mm)	F_X (N)	F_Y (N)	F_Z (N)
1	75 (1)	0.10 (1)	0.10 (1)	51 (1)	0.80 (1)	29.95	45.95	66.79
2	75 (1)	0.10 (1)	0.10 (1)	51 (1)	1.20 (2)	25.44	46.73	68.20
3	75 (1)	0.10 (1)	0.10 (1)	51 (1)	1.60 (3)	26.14	50.26	71.58
4	75 (1)	0.20 (2)	0.20 (2)	58 (2)	0.80 (1)	37.38	78.89	91.68
5	75 (1)	0.20 (2)	0.20 (2)	58 (2)	1.20 (2)	39.83	85.75	98.83
6	75 (1)	0.20 (2)	0.20 (2)	58 (2)	1.60 (3)	35.10	87.80	118.84
7	75 (1)	0.30 (3)	0.30 (3)	64 (3)	0.80 (1)	42.19	87.76	95.59
8	75 (1)	0.30 (3)	0.30 (3)	64 (3)	1.20 (2)	43.06	91.89	100.38
9	75 (1)	0.30 (3)	0.30 (3)	64 (3)	1.60 (3)	36.36	100.09	115.59
10	150 (2)	0.10 (1)	0.20 (2)	64 (3)	0.80 (1)	37.20	109.23	93.13
11	150 (2)	0.10 (1)	0.20 (2)	64(3)	1.20 (2)	36.00	122.46	101.55
12	150 (2)	0.10 (1)	0.20 (2)	64 (3)	1.60 (3)	35.40	134.34	103.76
13	150 (2)	0.20 (2)	0.30 (3)	51 (1)	0.80 (1)	39.07	80.98	103.12
14	150 (2)	0.20 (2)	0.30 (3)	51 (1)	1.20 (2)	29.07	87.01	107.07
15	150 (2)	0.20 (2)	0.30 (3)	51 (1)	1.60 (3)	24.05	94.08	120.78
16	150 (2)	0.30 (3)	0.10 (1)	58 (2)	0.80 (1)	48.11	145.45	119.19
17	150 (2)	0.30 (3)	0.10 (1)	58 (2)	1.20 (2)	43.46	150.73	126.71
18	150 (2)	0.30 (3)	0.10 (1)	58 (2)	1.60 (3)	48.99	177.75	137.18
19	226 (3)	0.10 (1)	0.30 (3)	58 (2)	0.80 (1)	27.02	80.42	75.71
20	226 (3)	0.10 (1)	0.30 (3)	58 (2)	1.20 (2)	27.82	81.10	82.45
21	226(3)	0.10 (1)	0.30 (3)	58 (2)	1.60 (3)	25.43	88.12	87.01
22	226 (3)	0.20 (2)	0.10 (1)	64 (3)	0.80 (1)	40.93	144.54	136.74
23	226 (3)	0.20 (2)	0.10 (1)	64 (3)	1.20 (2)	49.52	155.69	140.68
24	226 (3)	0.20 (2)	0.10 (1)	64 (3)	1.60 (3)	36.66	176.28	142.78
25	226 (3)	0.30 (3)	0.20 (2)	51 (1)	0.80 (1)	34.45	94.21	105.08
26	226 (3)	0.30 (3)	0.20 (2)	51 (1)	1.20 (2)	30.05	107.53	122.50
27	226 (3)	0.30 (3)	0.20 (2)	51 (1)	1.60 (3)	33.47	121.64	149.61

$\boldsymbol{b}$ and $\hat{\sigma}^2 = S_{\mathrm{res}}/(n - m - 1)$ is mutual independence, and, $b \sim N(\beta\ \sigma^2\ (x^{\mathrm{T}}x)^{-1})$, $E(b_j) = \beta_j, D(b_j) = c_{jj}\sigma^2$, where c_{jj} is a jth element along a diagonal line in matrix $(\boldsymbol{x}^{\mathrm{T}}\boldsymbol{x})^{-1}$.

Hence,

$$\left(b_j - \beta_j\right)/\sqrt{c_{jj}\sigma^2} \sim N(0, 1)$$

Under the condition of Eq. (12), utilizing $t = \frac{b_j}{\sqrt{c_{jj}S_{res}/(n-m-1)}}$ to test β_j is zero or not. Namely, tested independent variable x_j is significant or not.

3.1.4 Test of regression equation

Suppose

$$\mathrm{H}_0 : \beta_1 = \beta_2 = \ldots = \beta_{\mathrm{m}} = 0$$

Thus, the statistics F calculated according to regression and residual variance is compared and estimated after selecting confidence level and finding out the critical value of F in Table 5.

If the statistics $\mathrm{F} > \mathrm{F}_\alpha(m, n - m - 1)$, the assumption prerequisite is not supported, and namely, the regression equation is significant in confidence level $100(1-\alpha)\%$. Contrarily, the regression equation is significant.

3.2 Empirical model of three-component cutting forces

In this paper, the applicable conditions of the ORMEM and RSMQPEM are as follows:

1. Material of the workpiece is Cr12MoV.
2. Material of the tool is the PCBN which had an approximate chemical composition of 50% CBN.
3. Geometrical parameters are in Table 2.
4. Input variables should be v=75–226 m/min, f=0.10–0.30 mm/rev, a_{p}=0.10–0.30 mm, H=51–64±1 HRC, r_ε=0.80–1.60 mm, and $VB \leq 0.15$ mm.

3.2.1 Empirical model of the main cutting force $\boldsymbol{F}_Z$

The statistical software SPSS [25] was utilized to establish the regression model and calculate constants and regression coefficients of these models. After removing the variables with negligible regression coefficients, the ORMEM and RSMQPEM established of the main cutting force are described in Eqs. (13) and (14):

$$F_Z = 4.8067 v^{0.213} a_{\mathrm{p}}^{0.346} f^{-0.074} H^{0.608} r_\varepsilon^{0.230} \tag{13}$$

$$\begin{aligned} F_Z = {} & -62.17 + 0.674v + 59.999a_{\mathrm{p}} + 923.956f \\ & + 0.221H + 41.934r_\varepsilon + 1.06va_{\mathrm{p}} - 4.373vf + 0.028vr_\varepsilon \\ & -1724.17a_{\mathrm{p}}f + 116.25a_{\mathrm{p}}r_\varepsilon + 41.958fr_\varepsilon - 0.962Hr_\varepsilon \end{aligned} \tag{14}$$

The significance of the regression model was tested using the ANOVA method. Table 5 shows the ANOVA for the ORMEM and RSMQPEM of the three-component cutting forces. It also presents the sum of squares (SS), degrees of freedom (DF), mean squares (MS), calculated value of F_{cal}, and the critical value of $F_{0.05}$, in addition to the correlation coefficient R^2 (called R-squared).

The regression model is evaluated by an F test. If the calculated value of F_{cal} is greater than the critical value of $\mathrm{F}_{0.05}$ (95 % confidence level), the null hypothesis is rejected, which also implies that the model is significant. In addition, it indicates a good correlation between experimental and predicted values when R^2 comes closer to the value of unity.

It can be seen in Table 5 that the values of F_{cal} are more than $F_{0.05}$ for the two models, which implies that both of them are all significant. Moreover, the R^2 for the RSMQPEM is found to be greater than that for the ORMEM; namely, the

Table 5 ANOVA for empirical model of three-component cutting forces

Cutting forces	ORM							RSM					
	Model	SS	DF	MS	F_{cal}	$F_{0.05}$	R^2	SS	DF	MS	F_{cal}	$F_{0.05}$	R^2
F_Z	Regression	1.150	5	0.230	23.960	2.68	0.851	13,975.711	12	1,164.643	51.859	2.53	0.978
	Residual	0.202	21	0.010				314.408	14	22.458			
	Total	1.352	26					14,290.118	26				
F_Y	Regression	3.044	5	0.609	33.702	2.68	0.889	32,400.482	12	2,700.040	23.417	2.53	0.953
	Residual	0.379	21	0.018				1,614.236	14	115.303			
	Total	3.423	26					34,014.718	26				
F_X	Regression	0.918	5	0.184	16.023	2.68	0.792	1,230.713	12	102.559	7.150	2.53	0.860
	Residual	0.241	21	0.011				200.813	14	14.344			
	Total	1.159	26					1,431.525	26				

fitting degree for the RSMQPEM is greater than that for the ORMEM, which shows that the RSMQPEM can explain the variation to the extent of 0.978, while the ORMEM can explain the variation to the extent of only 0.851.

Now, ANOVA is utilized to determine and analyze the effect of parameters. According to the t distribution [21], $t_{0.01/2}$ is 2.831; $t_{0.05/2}$ is 2.080. The parameters are very significant if $|t|>t_{0.01/2}$. The parameters are significant if $t_{0.01/2}>|t|>t_{0.05/2}$. And, the parameters are not significant if $|t|<t_{0.05/2}$.

Table 6 ANOVA for the main and interaction effects of parameters on three-component cutting forces (F_Z, F_Y, and F_X)

Model	Factors	t	Test	P	Significance
F_Z	v	4.355	$\lvert t_v\rvert>t_{0.01/2}$	0.001	VS
	a_p	0.818	$\lvert t_{ap}\rvert<t_{0.05/2}$	0.427	NS
	f	7.938	$\lvert t_f\rvert>t_{0.01/2}$	0.000	VS
	H	0.285	$\lvert t_H\rvert<t_{0.05/2}$	0.780	NS
	r_ε	1.284	$\lvert t_{r\varepsilon}\rvert<t_{0.05/2}$	0.220	NS
	va_p	2.222	$t_{0.01/2}>\lvert t_{vap}\rvert>t_{0.05/2}$	0.043	S
	vf	−9.408	$\lvert t_{vf}\rvert>t_{0.01/2}$	0.000	VS
	vr_ε	0.607	$\lvert t_{vr\varepsilon}\rvert<t_{0.05/2}$	0.553	NS
	a_pf	−6.817	$\lvert t_H\rvert>t_{0.01/2}$	0.000	VS
	a_pr_ε	3.399	$\lvert t_{apr\varepsilon}\rvert>t_{0.01/2}$	0.004	VS
	fr_ε	1.227	$\lvert t_{fr\varepsilon}\rvert<t_{0.05/2}$	0.240	NS
	Hr_ε	−1.830	$\lvert t_{Hr\varepsilon}\rvert<t_{0.05/2}$	0.089	S
F_Y	v	1.189	$\lvert t_v\rvert<t_{0.05/2}$	0.254	NS
	a_p	2.047	$\lvert t_{ap}\rvert<t_{0.05/2}$	0.060	NS
	f	4.348	$\lvert t_f\rvert>t_{0.01/2}$	0.001	VS
	H	0.592	$\lvert t_H\rvert<t_{0.05/2}$	0.563	NS
	r_ε	−0.520	$\lvert t_{r\varepsilon}\rvert<t_{0.05/2}$	0.611	NS
	va_p	1.295	$\lvert t_{vap}\rvert<t_{0.05/2}$	0.216	NS
	vf	−3.598	$\lvert t_{vf}\rvert>t_{0.01/2}$	0.003	VS
	vr_ε	1.108	$\lvert t_{vr\varepsilon}\rvert<t_{0.05/2}$	0.287	NS
	a_pf	−5.269	$\lvert t_H\rvert>t_{0.01/2}$	0.000	VS
	a_pr_ε	0.939	$\lvert t_{apr\varepsilon}\rvert<t_{0.05/2}$	0.363	NS
	fr_ε	−0.947	$\lvert t_{fr\varepsilon}\rvert<t_{0.05/2}$	0.360	NS
	Hr_ε	0.643	$\lvert t_{Hr\varepsilon}\rvert<t_{0.05/2}$	0.531	NS
F_X	v	0.477	$\lvert t_v\rvert<t_{0.05/2}$	0.640	NS
	a_p	1.957	$\lvert t_{ap}\rvert<t_{0.05/2}$	0.071	NS
	f	2.142	$t_{0.01/2}>\lvert t_f\rvert>t_{0.05/2}$	0.050	S
	H	0.106	$\lvert t_H\rvert<t_{0.05/2}$	0.917	NS
	r_ε	−0.649	$\lvert t_{r\varepsilon}\rvert<t_{0.052}$	0.527	NS
	va_p	0.105	$\lvert t_{vap}\rvert<t_{0.05/2}$	0.918	NS
	vf	−1.664	$\lvert t_{vf}\rvert<t_{0.05/2}$	0.118	NS
	vr_ε	0.389	$\lvert t_{vr\varepsilon}\rvert<t_{0.05/2}$	0.703	NS
	a_pf	−2.409	$t_{0.01/2}>\lvert t_H\rvert>t_{0.05/2}$	0.030	S
	a_pr_ε	0.097	$\lvert t_{apr\varepsilon}\rvert<t_{0.05/2}$	0.924	NS
	fr_ε	−1.162	$\lvert t_{fr\varepsilon}\rvert<t_{0.05/2}$	0.265	NS
	Hr_ε	0.653	$\lvert t_{Hr\varepsilon}\rvert<t_{0.05/2}$	0.525	NS

VS very significant, *S* significant, *NS* not significant

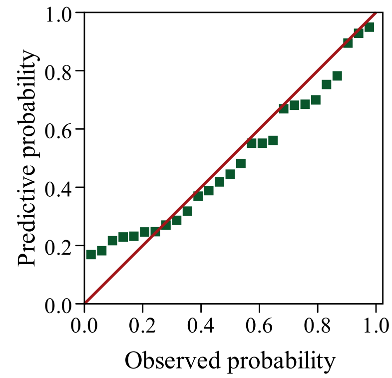

(a) Normal probability plot of residuals

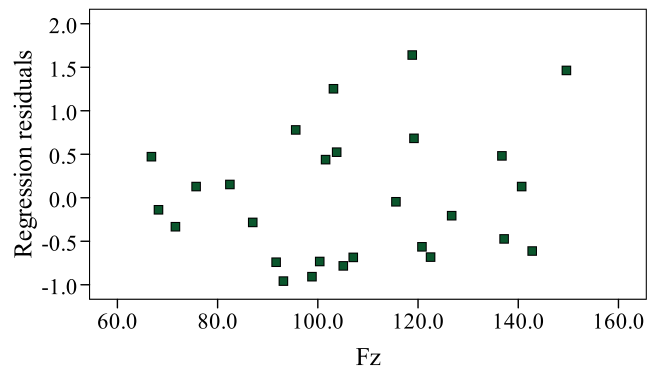

(b) Scatter diagram

Fig. 4 Residual plots for F_z. **a** Normal probability plot of residuals. **b** Scatter diagram

The ANOVA for the main and interaction effects of parameters on the three-component cutting forces is shown in Table 6. It is clear from the results in Table 6 that the cutting speed and feed are the two dominant factors determining the main cutting force; however, the effect of depth of cut, workpiece hardness, and nose radius on the main cutting force is less. Moreover, interaction effects of the cutting speed and depth of cut and the workpiece hardness and nose radius are significant followed by interaction effects of the cutting speed and feed,

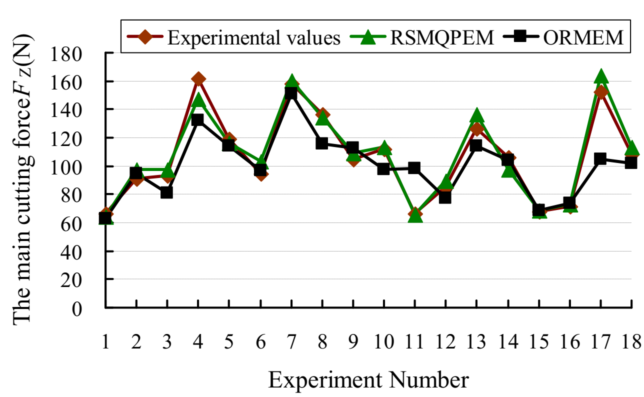

Fig. 5 Comparison between the ORMEM and RSMQPEM in the predicted main cutting forces

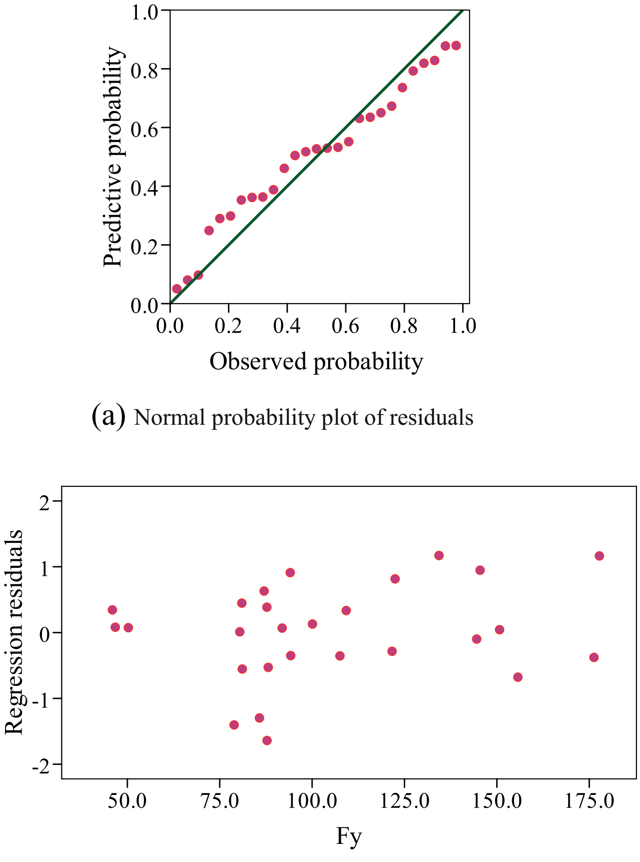

(a) Normal probability plot of residuals

(b) Scatter diagram

Fig. 6 Residual plots for F_Y

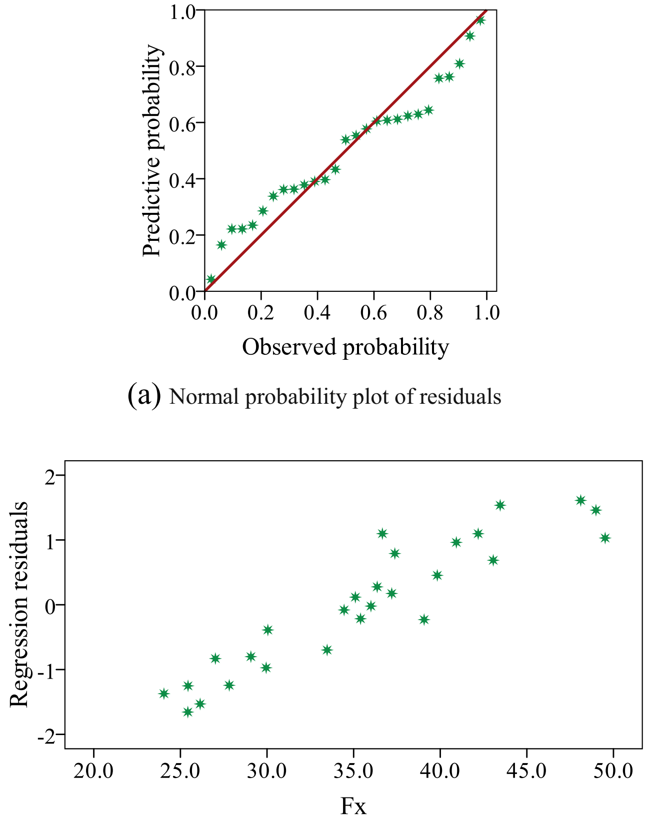

(a) Normal probability plot of residuals

(b) Scatter diagram

Fig. 8 Residual plots of RSM for F_X. **a** Normal probability plot of residuals. **b** Scatter diagram

depth of cut and feed, and depth of cut and radius, but the interaction effects of the cutting speed and nose radius and feed and nose radius are less.

The normal probability plot of residuals and scatter diagram for the main cutting force F_z in Fig. 4a, b can be utilized to further estimate the RSMQPEM. The predictions will be exact if the points are plotted on a straight line. Figure 4a shows that the residuals lie reasonably close to a straight line, which implies that the distribution of the errors is normal. Figure 4b indicates that the points present a random state and are all located in ±2σ. All of them show that the RSMQPEM is very good and there is no reason to doubt its correctness.

In order to understand the capability of the two models, the 18 experimental results were conducted by randomly selecting

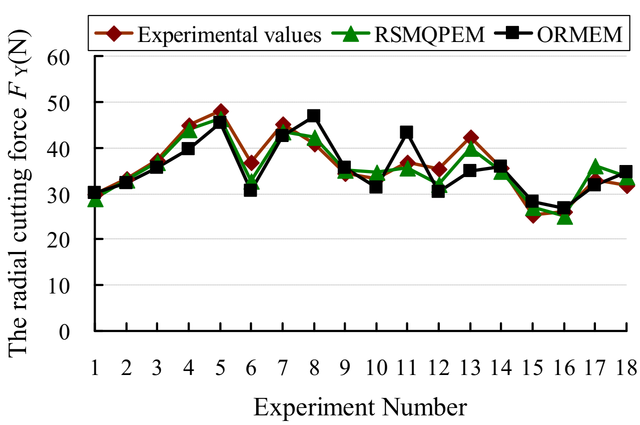

Fig. 7 Comparison between the ORMEM and RSMQPEM in the predicted radial cutting forces

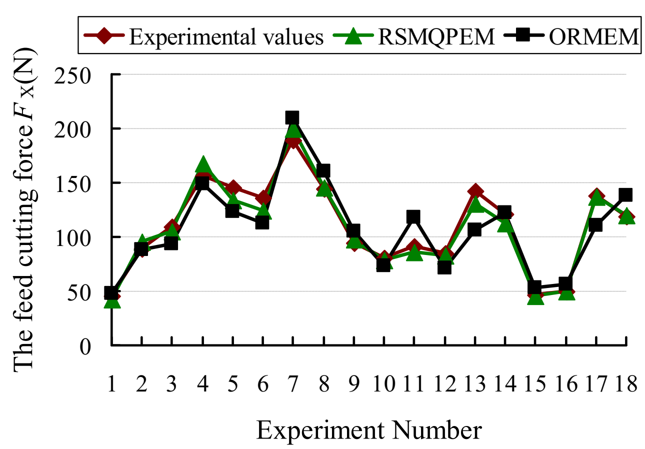

Fig. 9 Comparison between the ORMEM and RSMQPEM in the predicted feed cutting forces

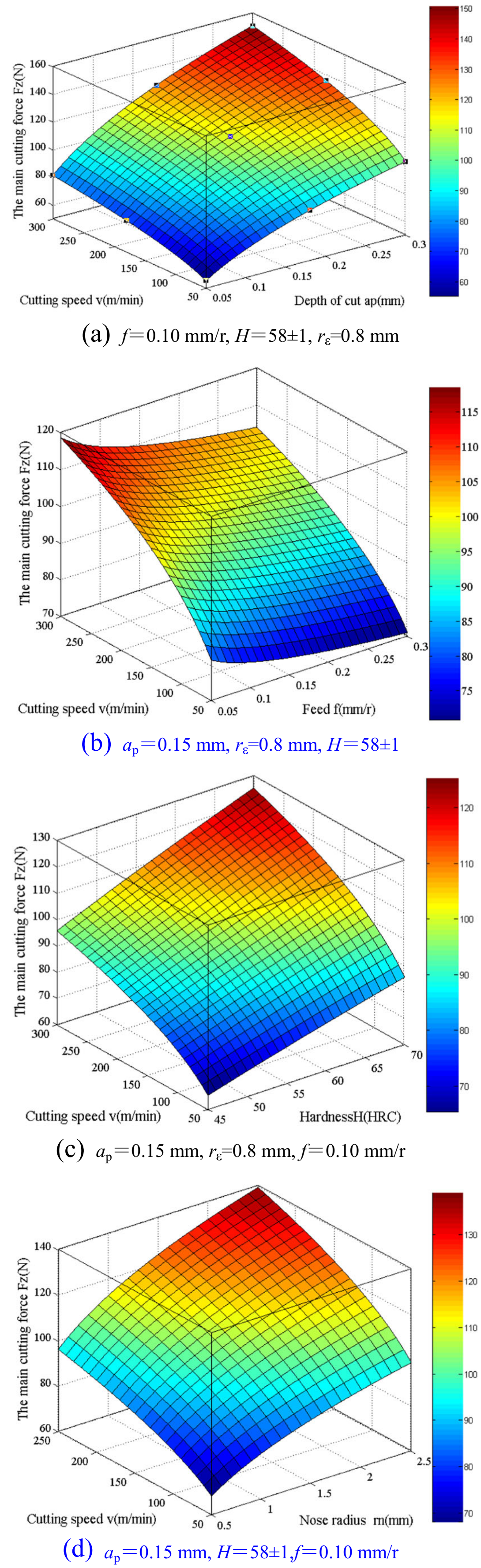

Fig. 10 Response surface plot for F_Z. **a** f=0.10 mm/rev, H=58±1, r_ε=0.8 mm. **b** a_p=0.15 mm, r_ε=0.8 mm, H=58±1. **c** a_p=0.15 mm, r_ε=0.8 mm, f=0.10 mm/rev. **d** a_p=0.15 mm, H=58±1, f=0.10 mm/rev

the input variables under the applicable conditions for the ORMEM and RSMQPEM. The absolute error can be determined with Eq. (15).

$$\Delta = \left| \frac{F_{expt} - F_{pred}}{F_{expt}} \right| * 100 \tag{15}$$

where
Δ (%) is the absolute error,
F_{exp} is the experimental value and
F_{pred} is the simulated value

The experimental results indicate that the absolute error of the ORMEM is 11.12 %, while that of the RSMQPEM is only 4.45 %, as shown in Fig. 5. As can be seen from the figure, it is obvious that the predicted values of the RSMQPEM closely match with the variation of the main cutting forces.

3.2.2 Empirical model of the radial cutting force $\boldsymbol{F_Y}$

Likewise, the established ORMEM and RSMQPEM of the radial cutting force are described in Eqs. (16) and (17):

$$F_Y = 0.0038067 v^{0.436} {a_p}^{0.366} f^{-0.157} H^{2.060} r_\varepsilon^{0.225} \tag{16}$$

$$\begin{aligned} F_Y = & -149.85 + 0.417v + 340.337a_p + 1146.687f \\ & + 1.04H - 38.483r_\varepsilon + 1.4va_p - 3.79vf + 0.114vr_\varepsilon \\ & - 3019.599a_pf + 72.792a_pr_\varepsilon - 73.375fr_\varepsilon + 0.765Hr_\varepsilon \end{aligned} \tag{17}$$

The significance of the regression model F_Y was also tested using the ANOVA method. It is clear in Table 5 that the values of F_{cal} are higher than $F_{0.05}$ for two models, which implies that both of them are all significant. Moreover, as shown in Table 5, the R^2 for the RSMQPEM is higher than that for the ORMEM, which implies the RSMQPEM is more significant than the ORMEM. The ANOVA for the main and interaction effects of cutting parameters on the radial cutting force F_Y is presented in Table 6. It is also clear in Table 6 that only the feed factor is very significant in determining the radial cutting force. Moreover, interaction effects of the cutting speed and feed and depth and cut and feed are very significant, but the interaction effects of the other parameters are less.

Likewise, in order to further estimate the RSMQPEM F_Y, the normal probability plot of residuals and scatter diagram are also presented in Figs 6a, b, respectively. It is clear from the Fig. 6a, b that the residuals lie reasonably close to a straight line, and the points present a random state and are all located in ±2σ, which is similar to the model F_Z. All of them show that the statistical model is very good.

Fig. 11 Response surface plot for F_Y. **a** f=0.10 mm/rev, H=58±1, r_ε=0.8 mm. **b** a_p=0.15 mm, r_ε=0.8 mm, H=58±1. **c** a_p=0.15 mm, r_ε=0.8 mm, f=0.10 mm/rev. **d** a_p=0.15 mm, f=0.10 mm/rev, H=58±1

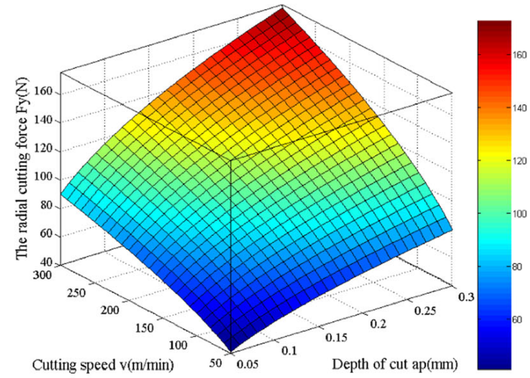

(a) f=0.10 mm/r, H=58±1, r_ε=0.8 mm

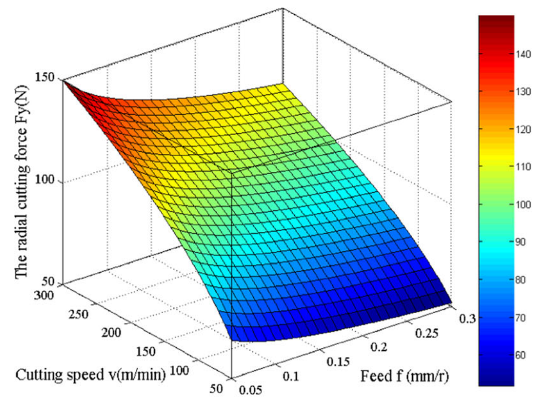

(b) a_p=0.15 mm, r_ε=0.8 mm H=58±1

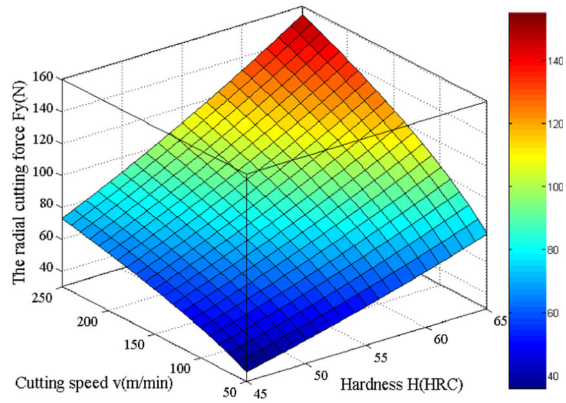

(c) a_p=0.15 mm, r_ε=0.8 mm, f=0.10 mm/r

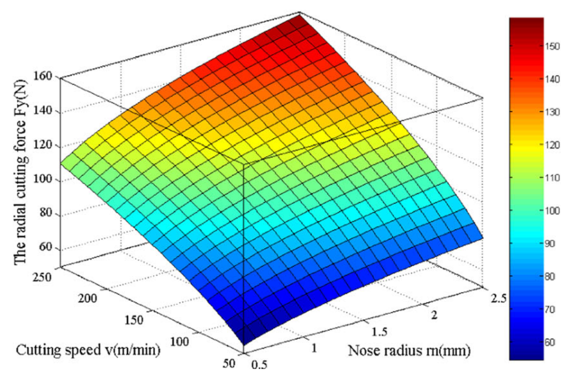

(d) a_p=0.15 mm, f=0.10 mm/r, H=58±1

As can be seen from Fig. 7, it is evident that the predicted results of the RSMQPEM do show much more accuracy by comparing the model output with the directly measured radial cutting forces. The experimental results indicate that the absolute error of the ORMEM is 13.01 %, while that of the RSMQPEM is only 4.75 %.

3.2.3 Empirical model of the feed cutting force F_X

Likewise, the developed ORMEM and RSMQPEM of the feed cutting force are described in Eqs. (18) and (19):

$$F_X = 0.31474 v^{-0.019} {a_p}^{0.262} f^{-0.143} H^{1.241} {r_\varepsilon}^{-0.167} \tag{18}$$

$$\begin{aligned} F_X = {} & 2.795 + 0.059v + 114.782a_p + 199.28f \\ & +0.066H - 16.926r_\varepsilon + 0.04va_p - 0.618vf \\ & +0.014vr_\varepsilon - 486.909a_p f + 2.646a_p r_\varepsilon \\ & -31.75 f r_\varepsilon + 0.274Hr_\varepsilon \end{aligned} \tag{19}$$

Table 5 shows that the calculated value of F_{cal} is larger than the critical value of $F_{0.05}$, and its R^2 is higher than the other. Thus, the reliability for the RSMQPEM is higher than that for the ORMEM. The ANOVA for the main and interaction effects of parameters on the feed cutting force is in Table 6. It can also be seen in Table 6 that only feed is the dominant factor determining the feed cutting force. Moreover, interaction effects of only the depth and cut and feed are significant.

The normal probability plot of residuals and scatter diagram for the RSMQPEM F_X are presented in Fig. 8a, b. It is obvious that distribution characteristics of the figure are similar to the model F_Z and F_Y; hence, the RSMQPEM for F_Y is very good.

Figure 9 represents a comparison between the experimental results and predicted values of the ORMEM and RSMQPEM for the feed cutting forces. The experimental results show that the absolute error of the ORMEM is 8.15 %, while that of the RSMQPEM is only 4.49 %. From the analysis of this figure, it can be asserted that the developed RSMQPEM gives closer correlation with experimental results.

3.3 Influence of process parameters on three-component cutting forces

The influences of process parameters on three-component cutting forces were analyzed above by ANOVA. Now, the complex RSMQPEM is visualized via 3-day plots. In each plot, two parameters are varied, and the others are to remain constant. The effects of parameters on three-component

Fig. 12 Response surface plot for F_X. **a** f=0.10 mm/rev, H=58±1, r_ε=0.8 mm. **b** a_p=0.15 mm, r_ε=0.8 mm, H=58±1. **c** a_p=0.15 mm, r_ε=0.8 mm, f=0.10 mm/rev. **d** a_p=0.15 mm, f=0.10 mm/rev, H=58±1

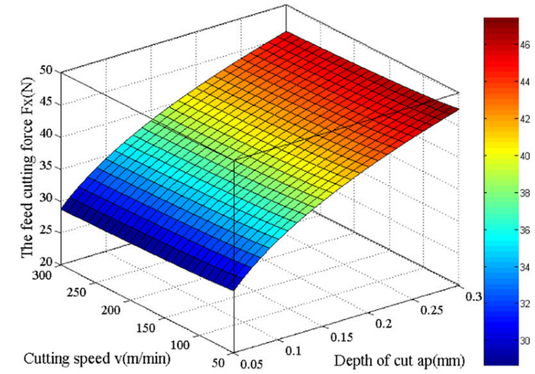

(a) f=0.10 mm/r, H=58±1, r_ε=0.8 mm

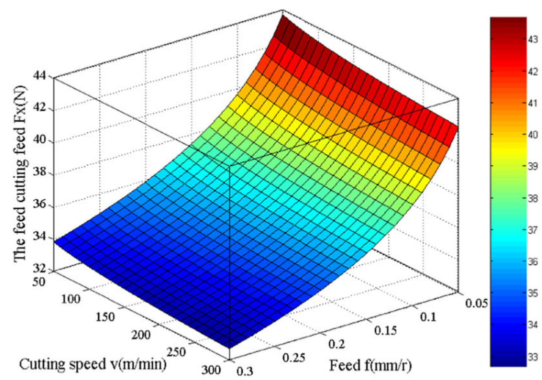

(b) a_p=0.15 mm, r_ε=0.8 mm H=58±1

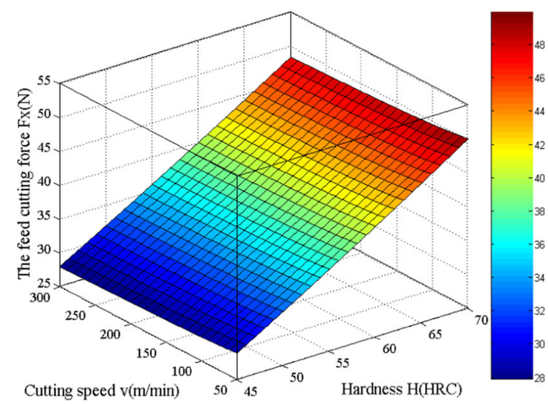

(c) a_p=0.15 mm, r_ε=0.8 mm, f=0.10 mm/r

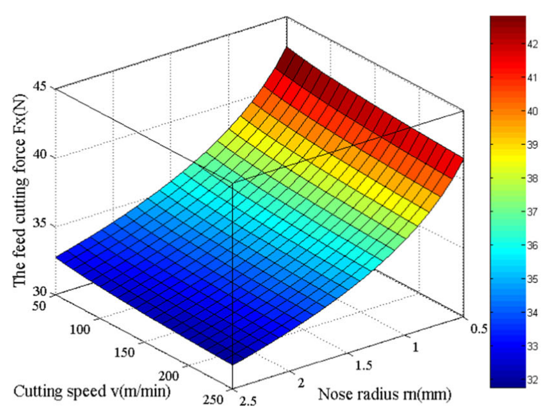

(d) a_p=0.15 mm, f=0.10 mm/r, H=58±1

cutting forces are simulated by utilizing an available software package (Matlab).

3.3.1 Influence of process parameters on the main cutting force

Figure 10a–d presents interaction effects between the cutting speed and the other factors on the main cutting force in the case of FDHT of hardened steel tool (58±1 HRC). It can be seen from the 3-day plots (Fig. 10a–d) that the main cutting force increases with the increase in the cutting speed, depth of cut, the workpiece hardness, and the nose radius, while it decreases with increments of the feed. It is also clear from this figure that the interaction effects between the cutting speed and feed on the main cutting force are the most significant.

3.3.2 Influence of process parameters on the radial cutting force

Figure 11a–d presents interaction effects between the cutting speed and the other factors on the radial cutting force. It can be seen from the 3-day plots that the radial cutting force sharply decreases and then gradually decreases with the increments of the feed, while as the cutting speed, depth of cut, workpiece hardness, and nose radius increase, the radial cutting force gradually increases. It is also clear from these figures that the interaction effects between the cutting speed and the feed on the main cutting force are the most significant.

3.3.3 Influence of process parameters on the feed cutting force

Figure 12a–d shows that the influence of the feed, depth of cut, workpiece hardness, and nose radius on the feed cutting force is very significant except that of the cutting speed. It can be observed from the 3-day plots that the feed cutting force slowly increases with the increase in the cutting speed, while it nonlinearly gradually increases and then sharply increases with the increments of depth of cut. However, it gradually decreases after a sudden decline with increments of the feed and nose radius, while it linearly increases with the rise of the workpiece hardness.

3.4 Optimization of cutting parameters

Optimization of cutting parameters is of great significance in not only increasing the machining efficiency but also improving the surface qualities and tool life. In this paper, an effort has been made to optimize the cutting parameters attaining the

Table 7 Optimized cutting parameters and the corresponding results of the three-component cutting forces

	v (m/min)	a_p (mm)	f (mm/rev)	H (HRC)	r_ε (mm)	n (N)
F_Z	75	0.10	0.10	51	0.8	64.6
	75	0.10	0.10	55	0.8	62.4
	75	0.10	0.10	60	0.8	59.7
	75	0.10	0.10	64	1.6	56.1
F_Y	75	0.10	0.10	51	0.8	42.2
	75	0.10	0.10	55	0.8	48.8
	75	0.10	0.10	60	0.8	57.1
	75	0.10	0.10	64	0.8	63.7
F_X	75	0.10	0.10	51	0.8	25.1
	75	0.10	0.10	55	0.8	27.1
	75	0.10	0.10	60	1.6	29.6
	75	0.10	0.10	64	1.6	31.7

lowest cutting forces. Here, the Eqs. (11), (17) and (19) are utilized to optimize the cutting parameters within the ranges given in this paper by an available software package (Matlab). The final results are summarized in Table 7.

4 Conclusions

In this paper, experimentations utilizing hardened tool steel AISI D2 at different hardness levels were conducted by using a tool insert PCBN. The influence of five factors (cutting speed, feed, depth of cut, workpiece hardness, and nose radius) on the three-component cutting forces in a FDHT process has been comprehensively analyzed by using ANOVA. And, the ORMEM and RSMQPEM for the three-component cutting forces by employing the five factors were developed by utilizing the ORM and RSM. The conclusions can be drawn from the above analysis:

1. ANOVA tests for two empirical models of three-component cutting forces show that the RSMQPEM is more significant than the ORMEM.
2. The experimental results show that the predicted values of RSMQPEM for three-component cutting forces are much more close to the experimental values than those of ORMEM. Therefore, it can be concluded that the developed RSMQPEM is more credible compared to the ORMEM in the considered parameter ranges. This model would be helpful in selecting the tool geometry and cutting conditions in FDHT of hardened tool steel AISI D2.
3. ANOVA tests for the main and interaction effects of parameters on three-component cutting forces show that the cutting speed and feed are of great influence on the main cutting force. And, all of the second interaction effects are very significant for the main cutting force except interactions of feed and nose radius and cutting speed and nose radius.
4. Among the main effect factors considered, the feed has more influence on the radial cutting force than the other factors. In addition, interaction effects of the cutting speed and feed and depth of cut and feed are very significant, but the interaction effects of the other parameters are less.
5. The influence of only feed is significant for the feed cutting force among five main effect factors. Moreover, the interaction effect of only the depth and cut and feed is significant.

Acknowledgments This investigation were supported by the Natural Science Foundation of China (51465028) and Scientific Research Project of Higher Schools of Gansu Province (2013A-131). The authors wish to thank Prof. J. Huang and the anonymous reviewers for their careful review and insightful comments that helped us improve this paper.

References

1. Gaitonde VN, Karnik SR, Figueira L, Paulo Davim J (2009) Analysis of machinability during hard turning of cold work tool steel (type: AISI D2). Mater Manuf Process 24(12):1373–1382
2. Klocke F, Brinksmeier E, Weinert K (2005) Capability profile of hard cutting and grinding processes. Ann CIRP 54(2):552–580
3. Ranganathan S, Senthilvelan T (2009) Behavior of machining parameters in hard turning of 316 stainless steel. Int J Manuf Sci Prod 10(2):137–145
4. Tang L, Huang J, Xie L (2011) Finite element modeling and simulation in dry hard orthogonal cutting AISI D2 tool steel with CBN cutting tool. Int J Adv Manuf Technol 53(1/2):1167–1181
5. Tang L, Gao C, Huang J, Lin X, Zhang J (2014) Experimental investigation of the three-component forces in finish dry hard turning of hardened tool steel at different hardness levels. Int J Adv Manuf Technol 70(9–12):1721–1729
6. More WC, Jiang W, Brown WD, Malshe AP (2006) Tool wear and machining performance of cBN-TiN coated carbide inserts and PCBN compact inserts in turning AISI4340 hardened steel. J Mater Process Technol 180(1–3):253–262
7. Sharma VS, Dhiman S, Sehgal R, Sharme SK (2008) Estimation of cutting forces and surface roughness for hard turning using neural networks. J Intell Manuf 19(4):473–483
8. Sieben B, Wagner T, Biermann D (2010) Empirical modeling of hard turning of AISI 6150 steel using design and analysis of computer experiments. Prod Eng 4(2):115–125
9. Ding T, Zhang S, Wang Y, Zhu X (2010) Empirical models and optimal cutting parameters for cutting forces and surface roughness in hard milling of AISI H13 steel. Int J Adv Manuf Technol 51(1):45–55
10. Gopalsamy B, Mondal B, Ghosh S (2009) Optimisation of machining parameters for hard machining: grey relational theory approach and ANOVA. Int J Adv Manuf Technol 45(11–12):1068–1086
11. Fnides B, Yallese MA, Mabrouki T, Rigal JF (2011) Application of response surface methodology for determining cutting force model in turning hardened AISI H11 hot work tool steel. Sadhana 36(1):109–123
12. Aouici H, Yallese MA, Chaoui K, Mabrouki T, Rigal JF (2012) Analysis of surface roughness and cutting force components in hard turning with CBN tool: prediction model and cutting conditions optimization. Measurement 45(3):344–353

13. Zhou AQ, Deng FY (2001) Experimental study on the heat treatment process for Cr12MoV steel. Die Mould Ind 000:55–57
14. Wang LJ, Miao B, Meng XX (2005) Analysis on the hardness and metallographic structure of Cr12MoV Steel under different heat treatment. Die Mould Ind 000:2–56
15. Dogra M, Sharma VS, Sachdeva A, Suri NM, Dureja JS (2010) Tool wear, chip formation and workpiece surface issues in CBN hard turning: a review. Int J Precis Eng Manuf 11(2):341–358
16. Wen D (2002) The mechanism and technology of hard turning with PCBN tool. Dalian University of Technology, Dissertation
17. Liu Z, Wan Y, Zhou J (2006) Tool materials for high speed machining and their fabrication technologies. Mater Mech Eng 30(5):1–4
18. Kilickap E, Huseyinoglu M, Yardimeden A (2011) Optimization of drilling parameters on surface roughness in drilling of AISI 1045 using response surface methodology and genetic algorithm. Int J Adv Manuf Technol 52(1–4):79–88
19. Natarajan U, Periyanan P, Yang S (2011) Multiple-response optimization for micro-endmilling process using response surface methodology. Int J Adv Manuf Technol 56(1–4):177–185
20. Tang Z (1997) Fundamental of mechanical manufacture. 1st edn. Machinery Industry Press, Beijing, p 11–12
21. Yuan Z, Song S (2009) Multivariate statistical analysis, 1st edn. 102, Beijing, pp 102–116
22. Fang K, Quan H (1988) Applied regression analysis, 1st edn. Science Press, Beijing, pp 202–206
23. Ren L (2009) Regression design and optimization, 1st edn. Science Press, Beijing, pp 232–256
24. Chen C, Chiang K (2011) Analyzing the design of vibration reduction with the rubber-layered laminates in the precision turning with a diamond cutting tool. Int J Adv Manuf Technol 19(1–4):101–116
25. Li X, Yin X (2008) SPSS economic and statistical analysis, 1st edn. China Statistics Press, Beijing, pp 261–289